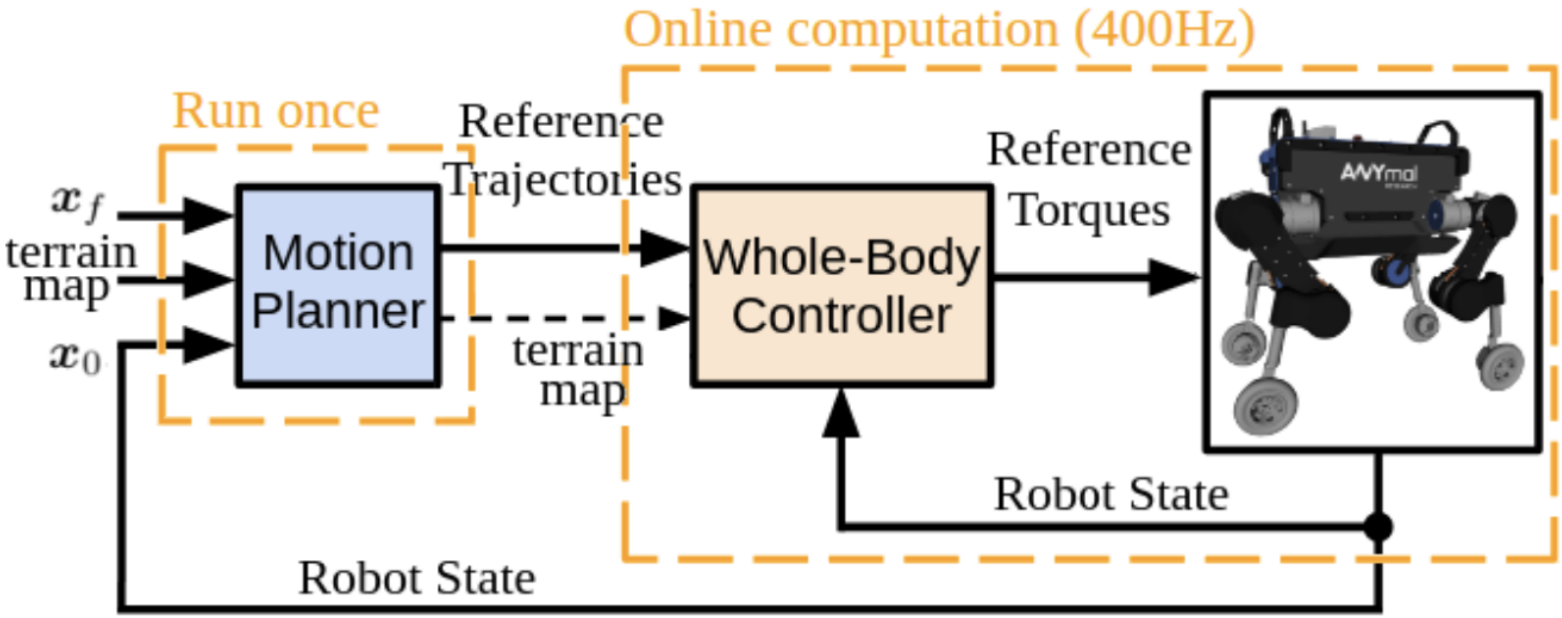

Fig. 8. Overview of the motion planning framework. The motion planner computes the reference trajectories for a specified time horizon that is given as input to the WBC, that computes the reference torques for the robot.

Trajectory Optimization for Wheeled-Legged Quadrupedal Robots Driving in Challenging Terrain

This section formalizes the TO problem for wheeled-legged robots and discusses its formulation as a NLP problem, as well as details of its collocation method. The goal of our motion planner is to solve an Optimal Control Problem (OCP) described as

$$\begin{aligned} &\text{find} && \boldsymbol{x}(t),\ \dot{\boldsymbol{x}}(t) \\ &\text{subject to} && \boldsymbol{x}(0)=\boldsymbol{x}_0, \quad \boldsymbol{x}(T)=\boldsymbol{x}_f, \\ &&& \boldsymbol{h}(\boldsymbol{x}(t),\dot{\boldsymbol{x}}(t),\ddot{\boldsymbol{x}}(t)) \geq \mathbf{0}, \\ &&& \boldsymbol{g}(\boldsymbol{x}(t),\dot{\boldsymbol{x}}(t),\ddot{\boldsymbol{x}}(t)) = \mathbf{0} \end{aligned}$$

where $\boldsymbol{x}(t)$ is the set of decision variables, given by the robot's CoM linear position and orientation (Euler angles), the wheels' contact positions and contact forces.

$$\boldsymbol{x}(t) = \begin{bmatrix} \boldsymbol{r}(t) & \boldsymbol{\theta}(t) & \boldsymbol{p}_i(t) & \boldsymbol{f}_i(t) \end{bmatrix}^T$$

The high-level user inputs are the initial and final state of the robot and the total time duration T of the trajectory. The duration T is defined based on the desired average speed for the robot's base.

$$\begin{aligned} &x(t) = a_0 + a_1 t + a_2 t^2 + a_3 t^3, \\ &a_i = f(x_k, \dot{x}_k, x_{k+1}, \dot{x}_{k+1}, \Delta T) \quad \forall\ k \in [0, n-1] \end{aligned} \tag{1}$$

1、Dynamic constrain

$$\begin{aligned} m\,{}^I\ddot{\boldsymbol{r}}(t) &= \sum_{i=1}^{4} {}^I\boldsymbol{f}_i(t) - m\,{}^I\boldsymbol{g} \\ \boldsymbol{I}\,{}^I\dot{\boldsymbol{\omega}}(t) + {}^I\boldsymbol{\omega}(t) \times \boldsymbol{I}\,{}^I\boldsymbol{\omega}(t) &= \sum_{i=1}^{4} {}^I\boldsymbol{f}_i(t) \times ({}^I\boldsymbol{r}(t) - {}^I\boldsymbol{p}_i(t)) \end{aligned} \tag{2}$$

2、kinematic constrain

$$-\boldsymbol{b} \ \leq\ \boldsymbol{R}_{BI}(\boldsymbol{\theta}(t))({}^I\boldsymbol{p}_i(t) - {}^I\boldsymbol{r}(t)) - {}^B\boldsymbol{p}_{in} \ \leq\ \boldsymbol{b}, \tag{3}$$

where $\boldsymbol{R}_{BI} \in \mathbb{R}^{3\times3}$ is the rotation matrix from the inertial frame to the base frame, ${}^B\boldsymbol{p}_{in} \in \mathbb{R}^3$ is the nominal position of the i^{th} wheel in the base frame and $\boldsymbol{b} = \begin{bmatrix} b_x & b_y & b_z \end{bmatrix}^T$ is the vector of parallelepiped dimensions.

3、Wheels' contact constraints

Firstly, all the wheels must be in contact with the ground, which is enforced by

$${}^Ip_i^z(t) = h_{terrain}({}^I\boldsymbol{p}_i^{x,y}(t)) \tag{4}$$

where $h_{terrain}$ is the continuous 2.5D height map of the terrain [25].

4、Wheels' force constrain

$$ {}^{I}\boldsymbol{f}_{n_i}(t) = {}^{C_i}\boldsymbol{f}_i^z(t) \geq 0, \tag{5}$$

where ${}^{C_i}\boldsymbol{f}_i^z(t)$ is the z component of the contact force on the i^{th} wheel expressed in the contact frame.

To ensure no slippage of the wheels' contact points, we constrain the tangential forces to remain inside the Coulomb friction cone defined by the terrain friction coefficient μ. In our implementation, the friction cone is approximated by a friction pyramid, which makes the constraint linear and thus, speeds up the computation. The constraint is given by

$$\begin{aligned} -\mu\, {}^{I}\boldsymbol{f}_{n_i}(t) \leq {}^{C_i}\boldsymbol{f}_i^x(t) \leq \mu\, {}^{I}\boldsymbol{f}_{n_i}(t) \\ -\mu\, {}^{I}\boldsymbol{f}_{n_i}(t) \leq {}^{C_i}\boldsymbol{f}_i^y(t) \leq \mu\, {}^{I}\boldsymbol{f}_{n_i}(t) \end{aligned} \tag{6}$$

Additionally, the traction forces are limited to a saturation value correspondent to the maximum torque of the wheel's motor, which is equivalent to limit the component of the contact force aligned with the rolling direction of the wheels:

$$ -\tau_{max}/w_r \leq {}^{C_i}\boldsymbol{f}_i^x(t) \leq \tau_{max}/w_r, \tag{7}$$

Since we constrain the contact forces in a way that there is no slippage on the wheels, the maximum traction force is defined by the maximum torque on the wheel's motor $\tau_{max} \in \mathbb{R}$ divided by the wheel's radius w_r.

5、 Stability constraint

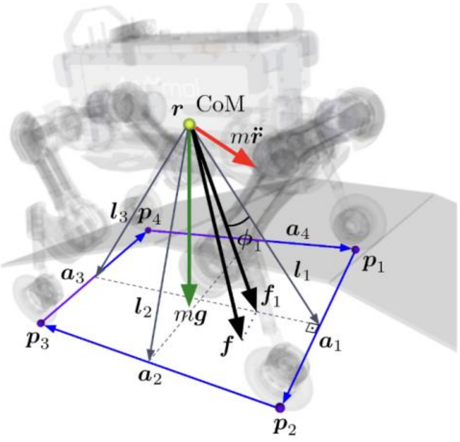

Fig. 6. Illustration of the Force-Angle Stability Measure for a quadrupedal robot, where $\boldsymbol{p}_i$ denotes the wheels' contact points; $\boldsymbol{a}_i$ denotes the tipover axes, defined as the vectors joining the contact points; $\boldsymbol{l}_i$ are the tipover axes normals, that intersect the tipover axis and the robot's CoM, which position is given by $\boldsymbol{r}$; $\boldsymbol{f}$ is the sum of all forces and angular loads acting on the CoM and $\boldsymbol{f}_1$ is the component of $\boldsymbol{f}$ that acts on the 1^{st} tipover axis; ϕ_1 is the stability angle w.r.t. to the first tipover axis. Same procedure is carried out to determine the correspondent $\boldsymbol{f}_i$ and ϕ_i for all tipover axes. All the vectors are represented in the inertial frame.

$$\beta = \min(\phi_i), \quad i = 1, \ldots, 4, \tag{9}$$

Trajectory Optimization for Wheeled-Legged Quadrupedal Robots using Linearized ZMP Constraints

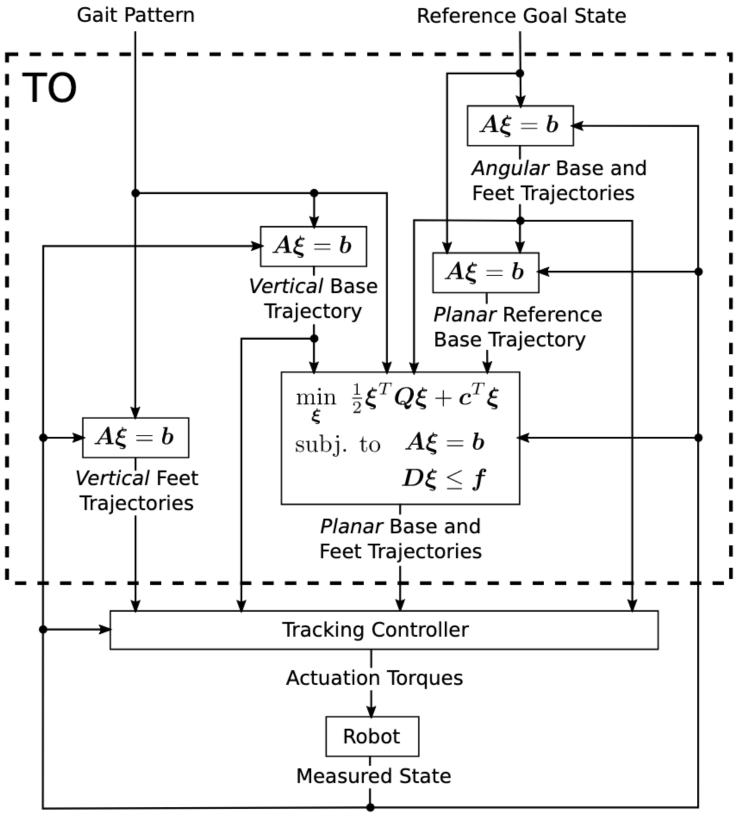

Fig. 3. Architecture of our cascaded TO. As explained in Section III, we are able to generate all trajectories by solving systems of linear equations (denoted as $\boldsymbol{A\xi} = \boldsymbol{b}$) or, in the case of the planar base and feet trajectories, a single QP problem. Note that, instead of a reference goal state, one may also directly provide the angular trajectories and the planar reference base trajectory.

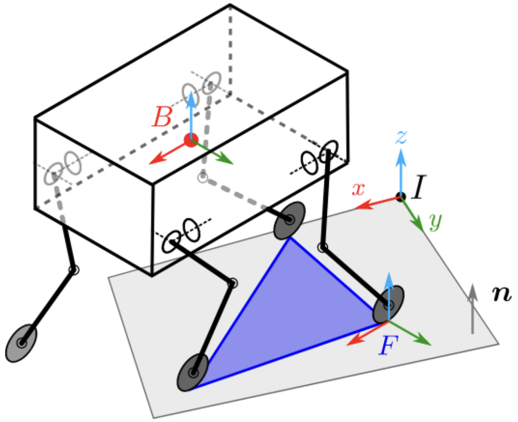

Fig. 2. Model of a wheeled-legged quadrupedal robot with massless legs and planar, nondeformable wheels. The current support polygon is shown in shaded blue. I denotes an inertial frame with z-axis collinear to the ground plane normal $\boldsymbol{n}$, and B the base frame with origin at the robot's CoM. We let the frame F be fixed at a leg's endpoint, i.e., the point that during stance is in contact with the ground (shown for the left hind (LH) leg only), and define this point as a leg's foot. This is a useful definition for our case, as we can model conventional point-contact feet and wheels simply by changing the kinematic constraints at F. Namely, by defining the z-axis of F to be aligned with the plane normal and the x-axis to be perpendicular to the wheel's rotation axis, the difference between the two becomes only whether F may have a non-zero velocity component along its x-direction.

Whole-Body MPC and Online Gait Sequence Generation for Wheeled-Legged Robots

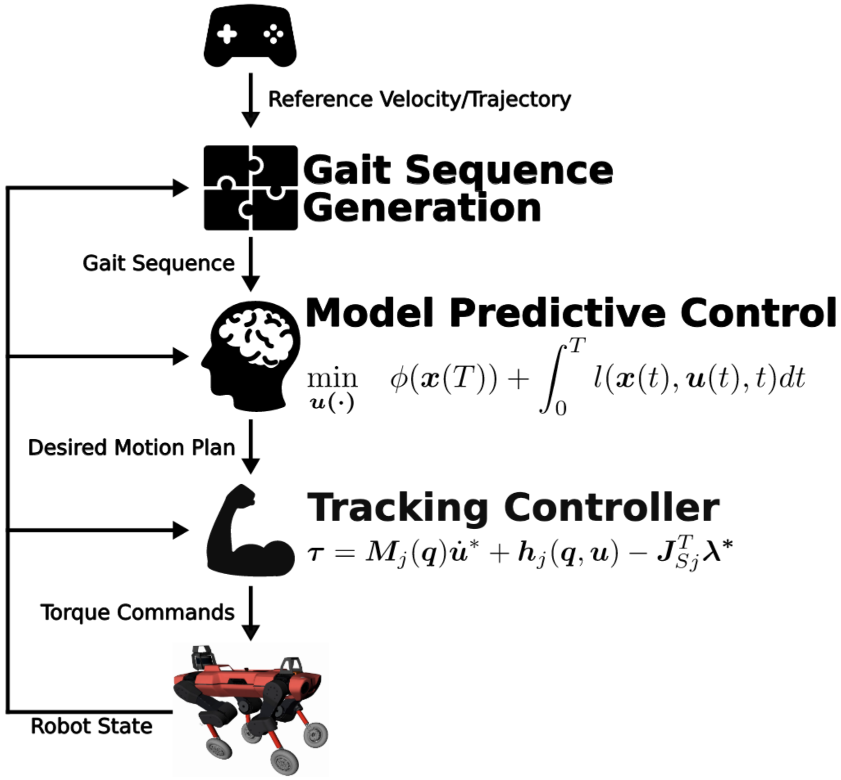

Fig. 2. Overview of the locomotion controller. The gait sequence generator automatically transforms reference trajectories from a higher-level planner or operator device into lift-off and touch-down sequences. These gait sequences are fed into the MPC that optimizes joint velocities and contact forces over a time horizon T. Finally, a tracking controller, e.g., [55], transforms the desired motion plan into torque references $\boldsymbol{\tau}$.

$$
\begin{aligned}
\underset{\boldsymbol{u}(\cdot)}{\text{minimize}} \quad & \phi(\boldsymbol{x}(T)) + \int_0^T l(\boldsymbol{x}(t), \boldsymbol{u}(t), t)\mathrm{d}t, && \text{(1a)}\\
\text{subjected to} \quad & \dot{\boldsymbol{x}}(t) = \boldsymbol{f}(\boldsymbol{x}(t), \boldsymbol{u}(t), t), && \text{(1b)}\\
& \boldsymbol{x}(0) = \boldsymbol{x}_0, && \text{(1c)}\\
& \boldsymbol{g}_1(\boldsymbol{x}(t), \boldsymbol{u}(t), t) = 0, && \text{(1d)}\\
& \boldsymbol{g}_2(\boldsymbol{x}(t), t) = 0, && \text{(1e)}\\
& \boldsymbol{h}(\boldsymbol{x}(t), \boldsymbol{u}(t), t) \geq 0. && \text{(1f)}
\end{aligned}
$$

$$
\begin{aligned}
\boldsymbol{x}(t) &= \begin{bmatrix}\boldsymbol{\theta}^T & \boldsymbol{p}^T & \boldsymbol{\omega}^T & \boldsymbol{v}^T & \boldsymbol{q}_j^T\end{bmatrix}^T \in \mathbb{R}^{12+n_j}, && \text{(2a)}\\
\boldsymbol{u}(t) &= \begin{bmatrix}\boldsymbol{\lambda}_E^T & \boldsymbol{u}_j^T\end{bmatrix}^T \in \mathbb{R}^{3n_e+n_j}, && \text{(2b)}
\end{aligned}
$$

where $n_j = 12$ and $n_e = 4$ are the number of joints (excluding the wheel) and legs. The elements $\boldsymbol{\theta}$, $\boldsymbol{p}$, $\boldsymbol{\omega}$, $\boldsymbol{v}$ and $\boldsymbol{q}_j$ of the state vector in (2a) refer to the torso's orientation in Euler angles, torso's position in world frame W, COM's angular rate, COM's linear velocity, and joint positions, respectively. Moreover, the control inputs in (2b) are the end-effector contact forces $\boldsymbol{\lambda}_E$ and joint velocities $\boldsymbol{u}_j$.

1、cost function

$$l(\boldsymbol{x}(t),\boldsymbol{u}(t),t)=\frac{1}{2}\tilde{\boldsymbol{x}}(t)^T\boldsymbol{Q}\tilde{\boldsymbol{x}}(t)+\frac{1}{2}\tilde{\boldsymbol{u}}(t)^T\boldsymbol{R}\tilde{\boldsymbol{u}}(t), \tag{3}$$

where $\boldsymbol{Q}$ is a positive semi-definite Hessian of the state vector error $\tilde{\boldsymbol{x}}(t)=\boldsymbol{x}(t)-\boldsymbol{x}_{\text{ref}}(t)$ and $\boldsymbol{R}$ is a positive definite Hessian of the control input vector error $\tilde{\boldsymbol{u}}(t)=\boldsymbol{u}(t)-\boldsymbol{u}_{\text{ref}}(t)$. The error vector require reference values for the whole-body, e.g., the torso's reference position and linear velocity are computed through an external reference trajectory[2] $\boldsymbol{r}_{B,\text{ref}}(t)$ of the torso B. The remaining variables of $\boldsymbol{x}(t)$ and $\boldsymbol{u}(t)$ are regularized to some nominal configuration.

2、dynamic constrain

$$\dot{\boldsymbol{\theta}}=\boldsymbol{T}(\boldsymbol{\theta})\boldsymbol{\omega}, \tag{4a}$$

$$\dot{\boldsymbol{p}}=\boldsymbol{R}_{WB}(\boldsymbol{\theta})\boldsymbol{v}, \tag{4b}$$

$$\dot{\boldsymbol{\omega}}=\boldsymbol{I}^{-1}\left(-\boldsymbol{\omega}\times\boldsymbol{I}\boldsymbol{\omega}+\sum_{i=1}^{n_e}\boldsymbol{r}_{E_i}(\boldsymbol{q}_j)\times\boldsymbol{\lambda}_{E_i}\right), \tag{4c}$$

$$\dot{\boldsymbol{v}}=\boldsymbol{g}(\boldsymbol{\theta})+\frac{1}{m}\sum_{i=1}^{n_e}\boldsymbol{\lambda}_{E_i}, \tag{4d}$$

$$\dot{\boldsymbol{q}}_j=\boldsymbol{u}_j, \tag{4e}$$

3、rolling constrain

$$\boldsymbol{\lambda}_{E_i}\in\mathcal{C}(\boldsymbol{n},\mu_C), \tag{5a}$$

$$\pi_{E_i,\perp}(\boldsymbol{v}_{E_i}(\boldsymbol{x},\boldsymbol{u}))=0, \tag{5b}$$

$$\boldsymbol{v}_{E_i}(\boldsymbol{x},\boldsymbol{u})\cdot\boldsymbol{n}=0, \tag{5c}$$

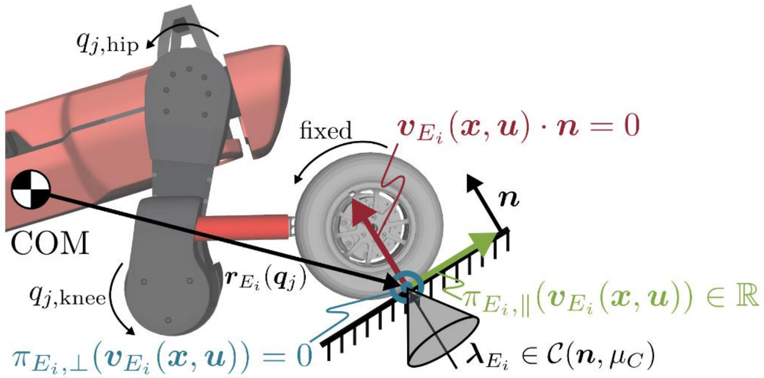

Fig. 3. Sketch of the rolling constraint with the underlying wheel model as a moving point contact with a fixed joint position. The image shows each direction of the end-effector velocity $\boldsymbol{v}_{E_i}(\boldsymbol{x},\boldsymbol{u})$, end-effector contact position $\boldsymbol{r}_{E_i}(\boldsymbol{q}_j)$, and friction cone constraint $\boldsymbol{\lambda}_{E_i}\in\mathcal{C}(\boldsymbol{n},\mu_C)$.

4、Gait Sequence Generation

By defining the utility as an ellipse, we can distinguish the decay along and lateral to the rolling direction. Therefore, the leg's utility $u_i(t)\in[0,1]$ is defined as

$$u_i(t)=1-\sqrt{\left(\frac{\pi_{E_i,\parallel}(\tilde{\boldsymbol{r}}_{E_i}(t))}{\lambda_{\parallel}}\right)^2+\left(\frac{\pi_{E_i,\perp}(\tilde{\boldsymbol{r}}_{E_i}(t))}{\lambda_{\perp}}\right)^2}, \tag{7}$$

2) Gait Timings Generation: The leg remains in contact as long as its utility $u_i(t)$ remains above a certain threshold $\bar{u}\in[0,1]$. If a leg's utility falls below the threshold, i.e., the leg is close to its workspace limits, then this leg is recovered by a swing phase with constant swing duration. Similar to [53], a multi-layered swing generator is proposed to achieve meaningful leg coordination:

1) **Utility Generation.** Calculate the utility for all legs $u_i(t)$ over a time horizon T.
2) **Utility Check.** Find the time t^* when $u_i(t)<\bar{u}$ and give legs with the lowest utility priority to add a swing phase with constant swing duration at time t^*.
3) **Neighboring Legs Check.** A swing phase is added if the neighboring legs[3] are not swinging. Otherwise, the swing phase is postponed until the neighboring legs are in contact—such an approach constrains the gaits to pure driving, hybrid static, and hybrid trotting gaits.

Keep Rollin' – Whole-Body Motion Control and Planning for Wheeled Quadrupedal Robots

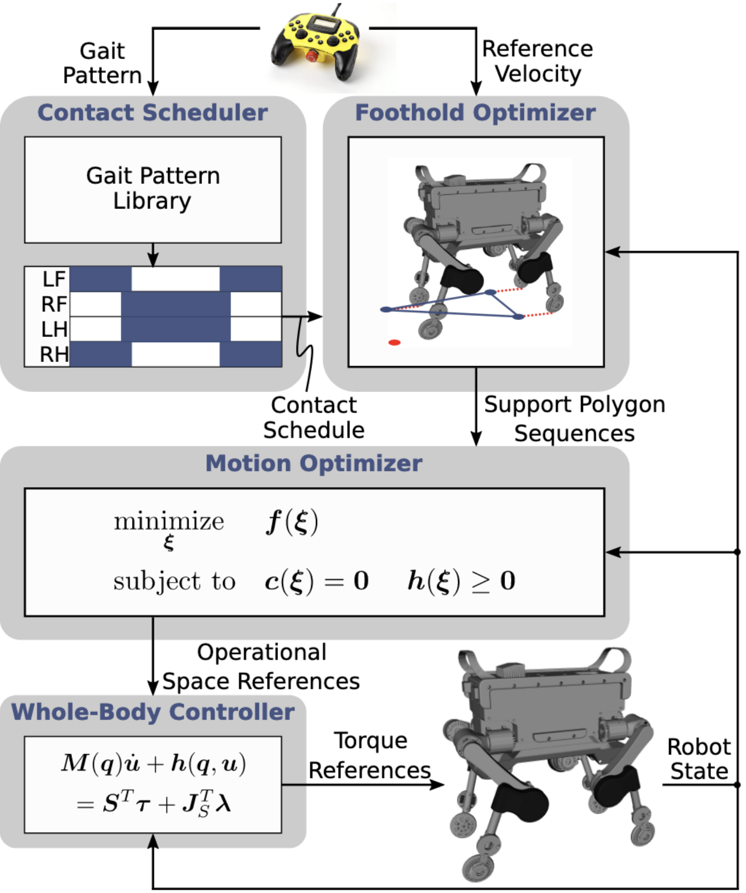

Fig. 3. The motion planner is based on a 3D ZMP approach which takes into account the support polygon sequence and the state of the robot. The hierarchical WBC which optimizes the whole-body accelerations and contact forces tracks the operational space references. Finally, torque references are sent to the robot.

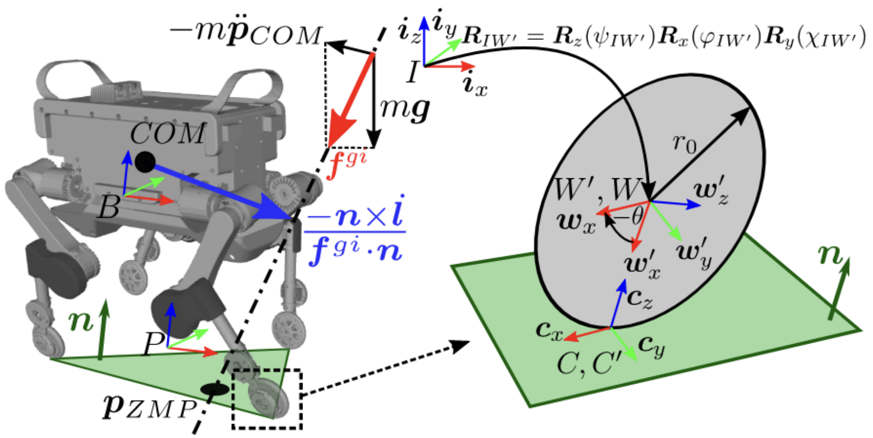

Fig. 2. The figure illustrates a sketch of the wheeled quadrupedal robot ANYmal and the wheel model used to derive the rolling constraint (3). **Left figure:** As discussed in [17], we define a plan frame P which is used as a reference frame in our motion planner. The red and blue arrows visualize the gravito-inertial wrench of the 3D ZMP model described in Section III-C3. **Right figure:** We differentiate between the leg-fixed and wheel-fixed coordinate frames at the wheel. The *leg-fixed* wheel frame W' and contact frame C' do not depend on the joint angle θ of the wheel. In contrast, the *wheel-fixed* wheel frame W' and contact frame C' depend on the joint angle θ of the wheel. Both contact frames are aligned with the local estimation of the terrain normal $\boldsymbol{n}$ and the rolling direction $\boldsymbol{c}_x$ of the wheel.

1、 Motion Optimizer :

$$\begin{aligned} \underset{\boldsymbol{\xi}}{\text{minimize}} \quad & \boldsymbol{f}(\boldsymbol{\xi}) \\ \text{subject to} \quad & \boldsymbol{c}(\boldsymbol{\xi}) = \mathbf{0}, \qquad \boldsymbol{h}(\boldsymbol{\xi}) \geq \mathbf{0}, \end{aligned} \tag{4}$$

TABLE I
THE TABLE LISTS THE COSTS AND CONSTRAINTS OF THE MOTION OPTIMIZATION PROBLEM BASED ON [17].

Type	Task	Purpose
Objective	Minimize COM acceleration	Smooth motions
Objective	Minimize deviation to previous solution $\boldsymbol{\xi}_{prev}$	Smooth motions
Objective	Track a high-level reference trajectory $\boldsymbol{\pi}$ (path regularizer) $\forall\,\boldsymbol{\xi}$	Reference tracking
Soft constraint (lin.-quad.)	Minimize deviation to initial & final conditions $\forall\,\boldsymbol{\xi}$	Disturbance rejection & reference tracking
Soft constraint (lin.-quad.)	Limit overshoots $\forall\,\boldsymbol{\xi}^z$	Avoid kinematic limits of legs
Constraint (lin. eq.)	Junction constraints $\forall$ pairs of adjacent splines $k,\ k+1\ \forall\,\boldsymbol{\xi}$	Continuity
Constraint (lin. ineq.)	Push Contact Constraints	Legs can only push the ground
Constraint (nonlin. ineq.)	ZMP criterion	Stability
Soft constraint (nonlin.)	Soften initial ZMP constraints	Relaxation

1、ZMP inequality constraint:

$$\begin{bmatrix} p & q & 0 \end{bmatrix} \boldsymbol{p}_{ZMP} + r \geq 0, \tag{5}$$

2、 Deformation of support polygons while driving :

$$\boldsymbol{p}_{\tau,i} = \boldsymbol{p}_{0,i} + \boldsymbol{R}(\tau\boldsymbol{\omega}_B^{ref}) \frac{1}{\omega_{B,z}^{ref}} \begin{bmatrix} \sin(\omega_{B,z}^{ref}\tau) & -1+\cos(\omega_{B,z}^{ref}\tau) & 0 \\ 1-\cos(\omega_{B,z}^{ref}\tau) & \sin(\omega_{B,z}^{ref}\tau) & 0 \\ 0 & 0 & 0 \end{bmatrix} \boldsymbol{v}_B^{ref}, \tag{6}$$

where $\boldsymbol{p}_{0,i} \in \mathbb{R}^3$ is the current foothold position. If $\omega_{B,z}^{ref} \approx 0$, the solution becomes $\boldsymbol{p}_{\tau,i} = \boldsymbol{p}_{0,i} + \tau\boldsymbol{v}_B^{ref}$.

1、 whole-body controller:

The WBC is formulated as a cascade of QP problems composed of linear equality and inequality tasks, which are solved in a strict prioritized order [30]. A task T_p with priority p is defined by

$$T_p : \begin{cases} \boldsymbol{W}_{eq,p}(\boldsymbol{A}_p\boldsymbol{\xi} - \boldsymbol{b}_p) = \boldsymbol{0} \\ \boldsymbol{W}_{ineq,p}(\boldsymbol{D}_p\boldsymbol{\xi} - \boldsymbol{f}_p) \leq \boldsymbol{0} \end{cases}, \tag{8}$$

2、Nonholonomic rolling constraint

$$\begin{bmatrix} \boldsymbol{J}_S & \boldsymbol{0}_{3n_c \times 3n_c} \end{bmatrix} \boldsymbol{\xi}_d = -\dot{\boldsymbol{J}}_S \boldsymbol{u} + \begin{bmatrix} {}_I\ddot{\boldsymbol{r}}_{IC_1}^T & \dots & {}_I\ddot{\boldsymbol{r}}_{IC_{n_c}}^T \end{bmatrix}^T, \tag{9}$$

3、COM linear and angular motion tracking

$$\begin{aligned} \begin{bmatrix} \boldsymbol{J}_{C_i'} & \boldsymbol{0}_{3n_c \times 3n_c} \end{bmatrix} \boldsymbol{\xi}_d = & \boldsymbol{R}_{IP}({}_P\ddot{\boldsymbol{r}}_{IC_i'}^d + \boldsymbol{K}_p({}_P\boldsymbol{r}_{IC_i'}^d - {}_P\boldsymbol{r}_{IC_i'}) \\ & + \boldsymbol{K}_d({}_P\dot{\boldsymbol{r}}_{IC_i'}^d - {}_P\dot{\boldsymbol{r}}_{IC_i'})) - \dot{\boldsymbol{J}}_{C_i'}\boldsymbol{u}, \end{aligned} \tag{10}$$

4、Swing wheel rotation minimization:

$$\begin{bmatrix} \boldsymbol{S}_{W_i} & \boldsymbol{0}_{3n_c \times 3n_c} \end{bmatrix} \boldsymbol{\xi}_d = -k_d \dot{\theta}_i, \tag{11}$$

where $\boldsymbol{S}_{W_i} \in \mathbb{R}^{3n_c \times n_u}$ is a matrix which selects the row of $\boldsymbol{\xi}_d$ containing the wheel of leg i, k_d is a derivative gain, and $\dot{\theta}_i$ is the wheel's rotational speed.

5、Ground leg motion tracking:

$$\begin{aligned} \pi_{\boldsymbol{c}_x}(\begin{bmatrix} \boldsymbol{J}_{C_i'} & \boldsymbol{0}_{3n_c \times 3n_c} \end{bmatrix} \boldsymbol{\xi}_d) = & \pi_{\boldsymbol{c}_x}(\boldsymbol{R}_{IP}({}_P\ddot{\boldsymbol{r}}_{IC_i'}^d \\ & + \boldsymbol{K}_p({}_P\boldsymbol{r}_{IC_i'}^d - {}_P\boldsymbol{r}_{IC_i'}) + \boldsymbol{K}_d({}_P\dot{\boldsymbol{r}}_{IC_i'}^d - {}_P\dot{\boldsymbol{r}}_{IC_i'})) - \dot{\boldsymbol{J}}_{C_i'}\boldsymbol{u}), \end{aligned} \tag{12}$$

where $\pi_{\boldsymbol{c}_x}(\boldsymbol{a})$ is the projection of a vector $\boldsymbol{a}$ onto the vector $\boldsymbol{c}_x$.

6、Torque Generation

$$\boldsymbol{\tau}_d = \boldsymbol{M}_j(\boldsymbol{q})\dot{\boldsymbol{u}}^* + \boldsymbol{h}_j(\boldsymbol{q}, \boldsymbol{u}) - \boldsymbol{J}_{Sj}^T \boldsymbol{\lambda}^*, \tag{13}$$

where $\boldsymbol{M}_j(\boldsymbol{q})$, $\boldsymbol{h}_j(\boldsymbol{q}, \boldsymbol{u})$, and $\boldsymbol{J}_{Sj}$ are the lower rows of the equations of motion in (2) relative to the actuated joints.

Thank you